Egypt.J.Chem. **Vol. 63**, No. 3. pp. 939-951 (2020)

Egyptian Journal of Chemistry
http://ejchem.journals.ekb.eg/

Spectroscopic Characterization and XRD of Some New Metal Complexes with Dithranol in Presence of 8-hydroxyquinoline

S.A. Sadeek[1]*, S.M. Abd El-Hamid[1], N.G. Rashid[2]
[1]*Department of Chemistry, Faculty of Science, Zagazig University, Zagazig, Egypt.*
[2]*Ministry of Education, Babylon, Iraq.*

IN THE PRESENT work, dithranol (Dithr) reacts with Ni(II), Zn(II), Zr(IV), La(III), and Th(IV) in presence of heterocyclic ligand 8-hydroxyquinoline (8HQ) in acetone forming new mixed ligand complexes. The structures of the synthesized complexes were characterized by conventional techniques including melting point, molar conductivity, magnetic properties, elemental analyses, infrared, ultraviolet-visible, ^{1}H nuclear magnetic resonance, and X-ray powder diffraction (XRD) spectra, as well as thermogravimetric (TG) and differential thermogravimetric (DTG) analyses. The molar conductance values of the metal complexes in dimethyl sulphoxide (DMSO) indicated that the complexes were found to be electrolytes with different ratios. The magnetic susceptibility measurements for Ni(II) complex is 3.1 BM with distorted octahedral geometry. TG/DTG studies confirmed the chemical formula for these complexes and established the thermal decomposition processes ended with the formation of metal oxide contaminated with carbon atom. The infrared spectra of the complexes showed shift for ν(O-H) and ν(C=N) in all complexes, which indicated the coordination of oxygen atom of phenolic group and nitrogen atom of pyridine ring of 8HQ with metal ions. X-ray powder diffraction analysis of the compounds showed that Dithr, 8HQ, and their metal complexes display crystalline peaks except Zr(IV) and La(III) complexes.

Keywords: ^{1}H nuclear magnetic resonance, 8-hydroxyquinoline, Dithranol, TG/DTG, X-ray powder diffraction.

Introduction

Dithranol or anthralin (Scheme 1A) is a Hydroxyanthrone, anthracene derivative, medicine applied to the skin of people with psoriasis. It is available as creams, ointment or pastes in 0.1 to 2% strengths with different names (Drithocreme, Dithrocream, Zithranol-RR, Micanol, Psorlin, Dritho-Scalp, Anthraforte, Anthranol and Anthra scalp). The terms dithranol and anthralin are sometimes used synonymously. Dithranol has a slower onset of action in controlling psoriasis, typically several weeks, compared to glucocorticoid steroids, but is without the potential for rebound reaction on withdrawal. It cannot be used on the face or genitalia. There is some tentative evidence that anthralin might be useful for alopecia aerate [1, 2].

Dithranol is a synthetic compound whose precise mechanism of anti-psoriatic action is not yet fully understood. However, numerous studies have demonstrated anti-proliferative and anti-inflammatory effects of anthralin on psoriatic and normal skin [3-6]. The anti-proliferative effects of dithranol appear to result from both an inhibition of DNA synthesis as well as from its strong reducing properties. Recently, dithranol's effectiveness as an anti-psoriatic agent has also been in part attributed to its abilities to induce lipid peroxidation and reduce levels of endothelial adhesion molecules which are markedly elevated in psoriatic patients [7, 8]. Unlike retinoid and PUVA, dithranol doesn't inhibit liver microsomal enzyme activity; consequently, the likelihood of adverse drug interactions is greatly reduced when other agents are administered concomitantly with dithranol. More dithranol penetrates into impaired skin in 30 minutes than into intact skin during about 16 hours. For this reason weaker 0.1-0.5% preparations are applied overnight, but stronger 1-2% products are applied for between 30min and one hour depending up on the formulation [9].

*Corresponding author e-mail: s_sadeek@zu.edu.eg Tel.: +20 01220057510, Fax: +20 0553208213.
Received 13/5/2019; Accepted 5/8/2019
DOI: 10.21608/ejchem.2019.12638.1789

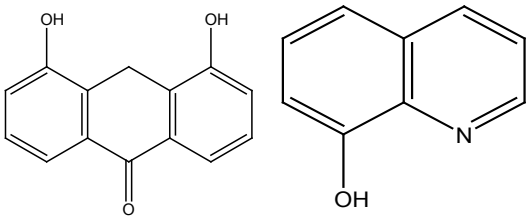

(A) (B)

Scheme 1 Structure of (A) dithranol (Dithr), (B) 8-hydroxyquinoline (8HQ).

8-hydroxyquinoline (Scheme 1B) is an organic compound with the formula C_9H_7NO. It is a derivative of the heterocyclic quinolone by placement of an OH group on carbon number 8. This light yellow compound is widely used commercially, although under avariety of names. 8-hydroxyquinoline was used to determine of magnesiumin Portland cement and similar materials [10].

In this work we report synthesis and characterization of new metal complexes derived from Dithranol (Dithr) and 8-hydroxyquinoline (8HQ). The structural characterization of the synthesized complexes was carried out using elemental analysis, infrared, electronic spectra, ^{1}H NMR, XRD and conductivity studies as well as thermal analysis (TG).

Experimental

Materials and reagents

All chemicals used for preparation of the complexes were of analytical reagent grade, commercially available from different sources and used without further purification. Dithranol used in this study was purchased from Obour Pharmaceutical Industrial Company. 8-hydroxyquinoline, $ZrOCl_2.8H_2O$ (99.9%), $Zn(CH3COO)_2.2H_2O$, $Ni(CH_3COO)_2.4H_2O$, $LaCl_3.7H_2O$ and $ThCl_4$ from Aldrich Chemical Co. All the chemicals and solvents were used as purchased without further purification.

Synthesis of mixed ligand metal complexes

The black solid complex $[Ni(Dithr)(8HQ)(H_2O)_2](CH_3COO)_2.H_2O$ (1) was prepared by mixing 1mmol (0.226 g) of Dithr and 1mmol (0.145 g) of 8HQ in 50ml acetone as a solvent with 1mmol (0.249 g) of $Ni(CH_3COO)_2.4H_2O$ in 20 ml acetone. The mixture was refluxed for 5 h and filtered off, washed several times with ethanol and dried under vacuum over anhydrous $CaCl_2$. The pale grey, grey, dark brown and the dark brown complexes, $[Zn(Dithr)(8HQ)(H_2O)_2](CH_3COO)_2$ (2), $[ZrO(Dithr)(8HQ)(H_2O)]Cl_2$ (3), $[La(Dithr)(8HQ)(H_2O)_2]Cl_3.3H_2O$ (4) and $[Th(Dithr)(8HQ)(H_2O)_2]Cl_4.4H_2O$ (5) were prepared in accordance with process described above by using $Zn(CH_3COO)_2.2H_2O$, $ZrOCl_2.8H_2O$, $LaCl_3.7H_2O$, $ThCl_4$, Dithr and 8HQ in 1:1:1 molar ratio.

Instruments

CHN analysis was carried on a Perkin Elmer CHN 2400. The percentages of the metal ions were determined gravimetrically by transforming the solid products into metal ions. The percentages of the metal ions were also estimated using an atomic absorption spectrometer. The spectrometer model PYE-UNICAM SP 1900 and fitted with the corresponding lamp was used. TGA-DTG measurements were run under N_2 atmosphere within the temperature range from room temperature to 1000°C using TGA-50H Shimadzu, the mass of sample was accurately weighted out in an aluminum crucible. FT-IR spectra were done on FT-IR 460 PLUS (KBr discs) in the range from 4000-400 cm^{-1}. ^{1}H NMR spectra in DMSO-d_6 were recorded on a Bruker 300 MHz NMR Spectrometer using tetramethyl silane (TMS) as the internal standard, and chemical shifts are expressed in δ (ppm). Absorbance measurements were conducted on a double beam spectrophotometer (T80UV/Vis) with wavelength range 190nm~1100 nm, spectral band width of 2nm. XRD patterns were determined by using a P analytical X'pent PRO with monochromatic Cu kα radiation with dissipation reflections registered for the 2θ angle between 4 and 79. Magnetic measurements were carried out on a Sherwood scientific magnetic balance using Gouy balance using Hg[Co(SCN)4] as calibrate. Melting points were determined on a Gallen Kamp electric melting point apparatus. Molar conductivities of the compounds in DMSO with concentrations of 1×10^{-3} M were measured on CONSORTK 410.

Results and Discussion

Dithr and 8HQ react with Ni(II), Zn(II), Zr(IV), La(III) and Th(IV) in presence of acetone to form solid complexes. The structures of the complexes were identified using elemental analysis, IR, UV-Vis., ^{1}H NMR spectra, XRD and TG/DTG analysis. The results listed in Table 1 indicated that the molar conductance values at room temperature for complexes

found in the range 150.00 to 270.44 S cm^2 mol^{-1}, which suggested that all the complexes found in electrolyte form and the complexes of Ni(II), Zn(II) and Zr(IV) showed 1:2 electrolyte, while La(III) and Th(IV) showed 1:3 and 1:4 electrolytes, respectively [11, 12]. Qualitative reactions agree well with the molar conductance data and revealed the presence of acetate and chloride ions as counter ions. Solutions of their complexes react with ferric chloride and silver nitrate giving red brown color of ferric acetate and white precipitate of silver chloride. The magnetic susceptibility measurements for Ni(II) complex found at 3.1 B.M., indicating distorted octahedral geometry [13].

FT-IR data and bonding

The significant FT-IR bands of the free ligands and their metal complexes (Fig. 1 and Table 2) were taken to detect the influence of a metal bonding on the ligand vibration in the complexes. The comparative IR spectral study of the free ligands (Dithr and 8HQ) and their complexes reveals the interesting coordination mode of the ligands during complex formation.

The ligands IR spectra showed a medium intensity broad bands at 3423 and 3433 cm^{-1} due to *ν*(O-H) [14]. The infrared spectra of the complexes showed the presence of the spectral absorption bands in the region 3419-3435 cm^{-1} corresponds to the ν(O-H) vibration in Dithr and 8HQ. The shift of *ν*(O-H) in all complexes indicate the coordination of phenolic group with the metal ions [15-18].

The band found at 1626 cm^{-1} in the infrared spectrum of 8HQ attributed to the stretching vibration of ν(C=N). Upon comparison of the IR spectra of the complexes with free ligand, the ν(C=N) shift to lower frequency values (1551 and 1575 cm^{-1}) confirming that the ligand molecule coordinated to metal ion through the nitrogen atom of pyridine ring [19]. The shift of ν(C=N) to lower values may indicate a decrease of C=N bond strength upon coordination. The possibility that the electron density on the nitrogen atom was decreased upon coordination to metal ions means a decrease in double bond character leading to a weaker C=N bond then, a lower frequency bond [20, 21].

TABLE 1. Elemental analysis and physico-analytical data for Dithr, 8HQ and their metal complexes.

Compounds M.Wt. (M.F.)	Yield%	Mp/ °C	Color	Found (Calcd.) (%)					Λ S cm^2 mol^{-1}
				C	H	N	M	Cl	
Dithr 226.23 ($C_{14}H_{10}O_3$)	-	180	Pale brown	74.22 (74.26)	4.40 (4.42)	-	-	-	10.2
8HQ 145.16 (C_9H_7NO)	-	76	White	73.87 (73.89)	4.76 (4.79)	9.56 (9.58)	-	-	5.7
(1) 602.21 ($NiC_{27}H_{29}NO_{11}$)	65.64	290	Dark brown	53.85 (53.87)	4.85 (4.87)	2.33 (2.36)	9.75 (9.77)	-	150.00
(2) 590.91 ($ZnC_{27}H_{27}NO_{10}$)	68.05	273	Pale grey	54.88 (54.90)	4.61 (4.64)	2.37 (2.39)	11.07 (11.09)	-	155.40
(3) 567.53 ($ZrC_{23}H_{19}NO_6Cl_2$)	74.2	281	Black	48.68 (48.71)	3.37 (3.39)	2.47 (2.50)	16.07 (16.09)	12.49 (12.53)	180.20
(4) 706.73 ($LaC_{23}H_{27}NO_9Cl_3$)	81.2	260	Grey	39.09 (39.11)	3.85 (3.89)	1.98 (2.00)	19.65 (19.68)	15.05 (15.07)	220.10
(5) 853.33 ($ThC_{23}H_{29}NO_{10}Cl_4$)	78.9	130	Dark brown	32.37 (32.39)	3.43 (3.46)	1.64 (1.66)	27.19 (27.21)	16.62 (16.65)	270.44

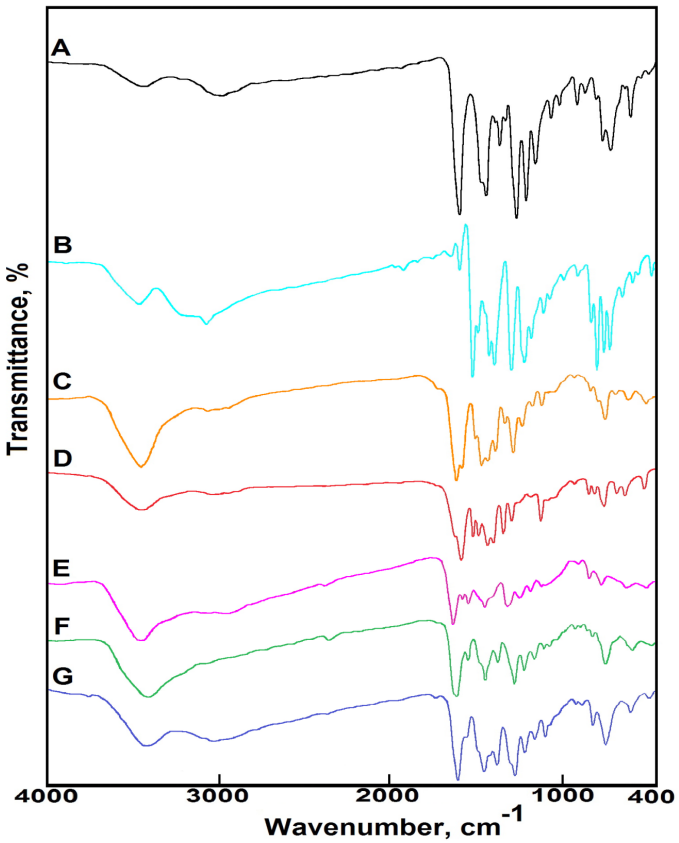

Fig. 1. Infrared spectra for (A) Dithr, (B) 8HQ, (C) (1), (D) (2), (E) (3), (F) (4) and (G) (5).

TABLE 2 Selected infrared absorption frequencies (cm^{-1}) of Dithr, 8HQ and their metal complexes.

Compounds	ν(O-H); phenolic and H_2O	ν(C=O)	ν(C=N)	ν (Zr=O)	ν(M-O) and ν(M-N)
Dithr	3423br	1603vs	-	-	-
8HQ	3433br	-	1626m	-	-
(1)	3435mbr	1604vs	1575w	-	680vw, 609w, 505w
(2)	3426br	1600sh	1567vs	-	663w, 616w, 505m
(3)	3419mbr	1602s	1551w	822w	607w, 588sh, 491w
(4)	3420mbr	1607vs	1560m	-	666sh, 592m, 500sh, 483vw
(5)	3422br	1604vs	1554vw	-	605m, 497vw

Keys: s= strong, w= weak, m= medium, br= broad, *ν*= stretching.

To ascertain the involvement of the phenolic group in chelation (Scheme 2), this requests to make a follow up of the stretching vibration bands of *ν*(C-O) in all complexes. The *ν*(C-O) bond stretch in case of free ligands shifted from 1093 cm^{-1} to 1078-1072 cm^{-1} in the complexes in addition to decrease of their intensities, pointing to the involvement of the phenolic oxygen in the chelation [21]. In turn, the strong band at 1660 cm^{-1} assigned to *ν*(C=O) of Dithr was upshifted in all complexes. This indicates the unparticipating of the carbonyl oxygen in chelation.

Also, the spectra of the isolated complexes showed a group of new bands with different intensities which characteristics for *ν*(M-O) and *ν*(M-N). The *ν*(M-O) and *ν*(M-N) bands observed at 680, 609, 505 cm^{-1} for Ni(II), at 663, 616 and 505 cm^{-1} for Zn(II), at 607, 588, 491 cm^{-1} for Zr(IV), at 666, 592, 500 and 483 cm^{-1} for La(III) and at 605 and 497 cm^{-1} for Th(IV), which are absent in the spectrum of Dithr and 8HQ.

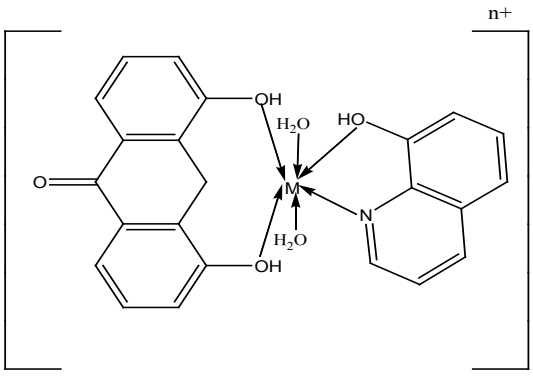

n=2 for Ni(II) and Zn(II)

n=3 for La(III)

n=4 for Th(IV)

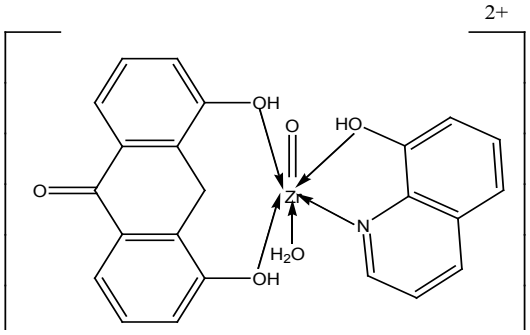

Scheme 2. The coordination mode of Ni(II), Zn(II), Zr(IV), La(III) and Th(IV) with Dithr and 8HQ.

UV–Visible spectra

The formation of mixed ligand complexes was confirmed by electronic absorption spectra which can be useful in structural determinations of chelates since they all absorb in this region. The electronic absorption spectra of ligands along with Ni(II), Zn(II), Zr(IV), La(III) and Th(IV) complexes from 200 to 800 nm are shown in Fig. 2 and listed in Table 3. Free Dithr and 8HQ showed bands at 262, 256 and at 355, 371, 300 nm which may be assigned to π-π^* and n-π^* transitions, respectively [22-24]. The shift of the absorption bands to higher or lower values and appearance of new bands in the spectra of the complexes is attributed to chelation of ligands. The decrease or increase of the absorption bands and appearance of new bands upon chelation could be caused by the following reasons. 1) The expected increase of the metal ions mass upon coordination. 2) The increase of electron density on metal ions by ligand. 3) Decrease of electron density on oxygen and nitrogen donor atoms (lone pair of electrons). The complexes of Ni(II), Zn(II), Zr(IV), La(III) and Th(IV) showed bands at 400, 398, 402, 398 and 396 nm, respectively, which may be assigned to ligand–metal charge transfer. Also, Ni(II) complex exhibit a d-d transition bands at 545 and 610 nm.

^{1}H NMR spectra

The suggested molecular structures of complexes also, proved by nuclear magnetic resonance (NMR) spectroscopy. The ^{1}H NMR spectra of the compounds in DMSO-d_6 (Fig. 3) displayed distinct signals with appropriate multiples, the signals assignments are given in Table 4. The ^{1}H NMR spectrum of Dithr showed peaks in the range 2.51-3.46 ppm and 6.85-7.59 ppm corresponding to the protons of–CH_2 and aromatic ring while the singlet peak at 12.04 ppm assigned to the OH proton. The ^{1}H NMR spectrum of 8HQ showed peaks in the range 7.10-8.85 ppm for the protons of aromatic ring and singlet peak at 10.5 ppm for the OH proton signal. Comparing the ^{1}H NMR spectra of the compounds showed the slightly changed for the main signals of complexes compared to the free ligands. Also, the ^{1}H NMR spectra for complexes exhibit new peak in the range 3.16-4.45 ppm, due to presence of water molecules in the complexes [25-27]. It is of interest to note that Baker and Sawyer did not extend their spectra to include the OH proton signal [28]. This occurs at 12.04 ppm downfield of TMS in the free Dithr and in solutions of Zn(II) complex (as an example) where it is considerably broadened by hydrogen bonding and disappears on addition of D_2O [28].

Thermal analysis

Thermo gravimetric analysis (TGA) of the compounds was performed, over the temperature range 25–1000^{o}C and the obtained data are presented in Table 5. Dithr, 8HQ and their complexes have been tested using TGA to study the stability of compounds. Dithr decomposed in one step with lose of $3C_4H_2$+2CO+H_2O+H_2 at 274 ^{o}C. The thermal degradation of 8HQ takes place at one degradation stage with maximum 176 ^{o}C and accompanied by a weight loss of 99.49% corresponding to loss of $2C_4H_2$+NH_3+CO, the pictorial representations are given in Fig. 4.

Complex (1) showed three weight loss events. The first step of decomposition occurs at 71 °C maximum with estimated mass loss 3.05% (calc. = 2.99%) corresponding to the loss of one hydrated water molecule. The second step of

decomposition carried out at 250°C with the loss of $4C_2H_2+NH_3+CO_2$ (found mass lose 27.22% (calc. = 27.43%). The final step recorded at 325°C with estimated mass loss of 39.12% (calc. = 39.23%), corresponds to loss of $2C_2H_6+C_2H_4+3CO+2O_2$ fragment leaving NiO+9C as the final residue. The overall weight loss amounted to 69.39% (calc. = 69.65%).

The TGA curves of (2) and (3) complexes showed two steps of decomposition. The first stage found at 73 and 99 °C maxima and the second step occurs at 327 and 330 °C. The total mass loss of weight at the end of decomposition is 67.29% and 67.61% (Calcd. 67.94% and 67.70%). The weight loss of the residue ZnO+9C and ZrO_2+5C (32.71% and 32.39%) matched with the theoretical values (32.06% and 32.30%).

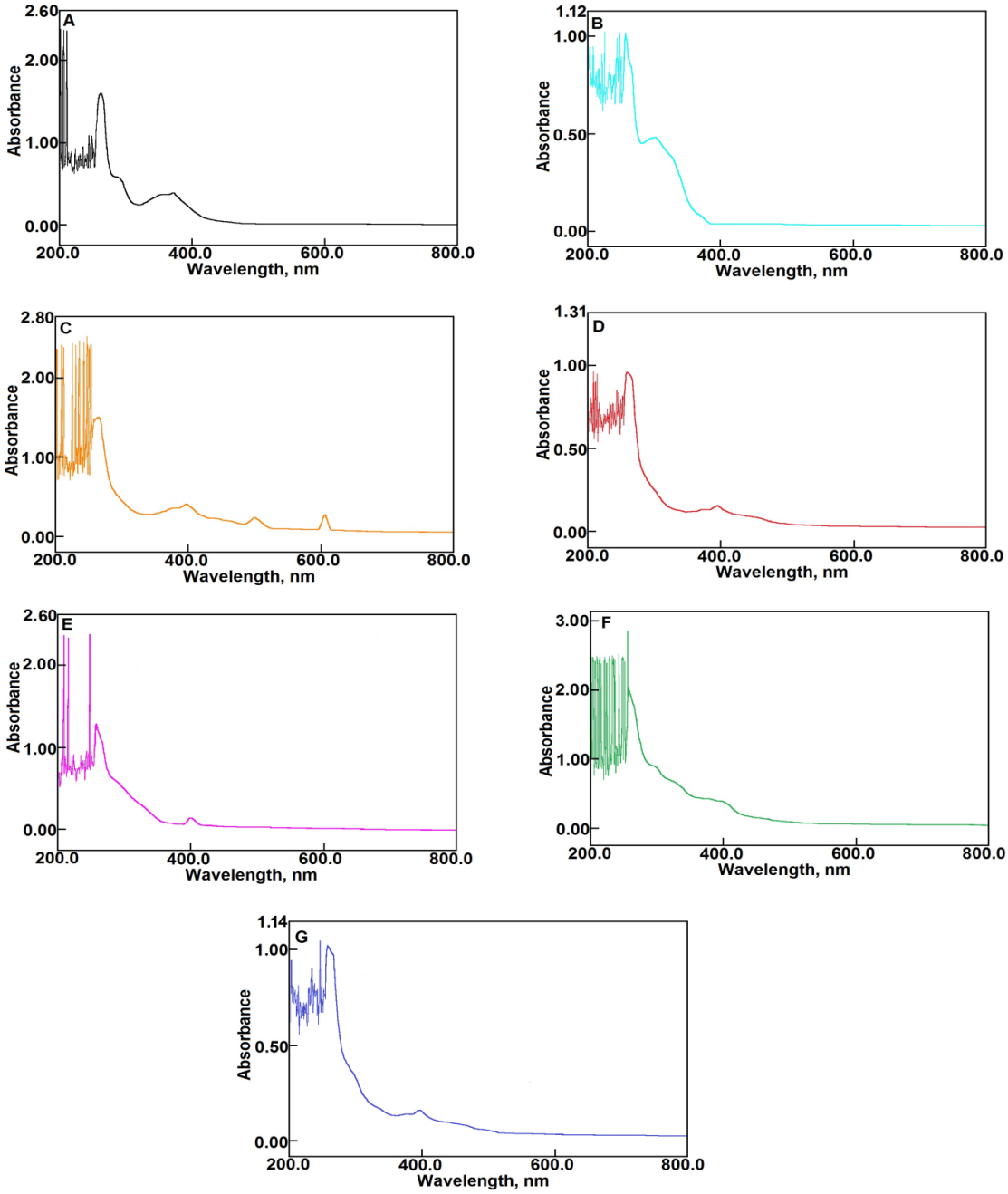

Fig. 2. Electronic absorption spectra for (A) Dithr, (B) 8HQ, (C) (1), (D) (2), (E) (3), (F) (4) and (G) (5).

TABLE 3. UV-Vis. spectra of Dithr, 8HQ, 1, 2, 3, 4 and 5 complexes.

Assignments (nm)	Dithr	8HQ	Mixed ligand complex with				
			1	2	3	4	5
π-π^* transitions	262	256	246	243 258	250	249 257	253
n-π^* transitions	355 371	300	379	273	305	284 309	282 375
Ligand-metal charge transfer	-	-	400	398	402	398	396
d-d transition	-	-	545 610	-	-	-	-

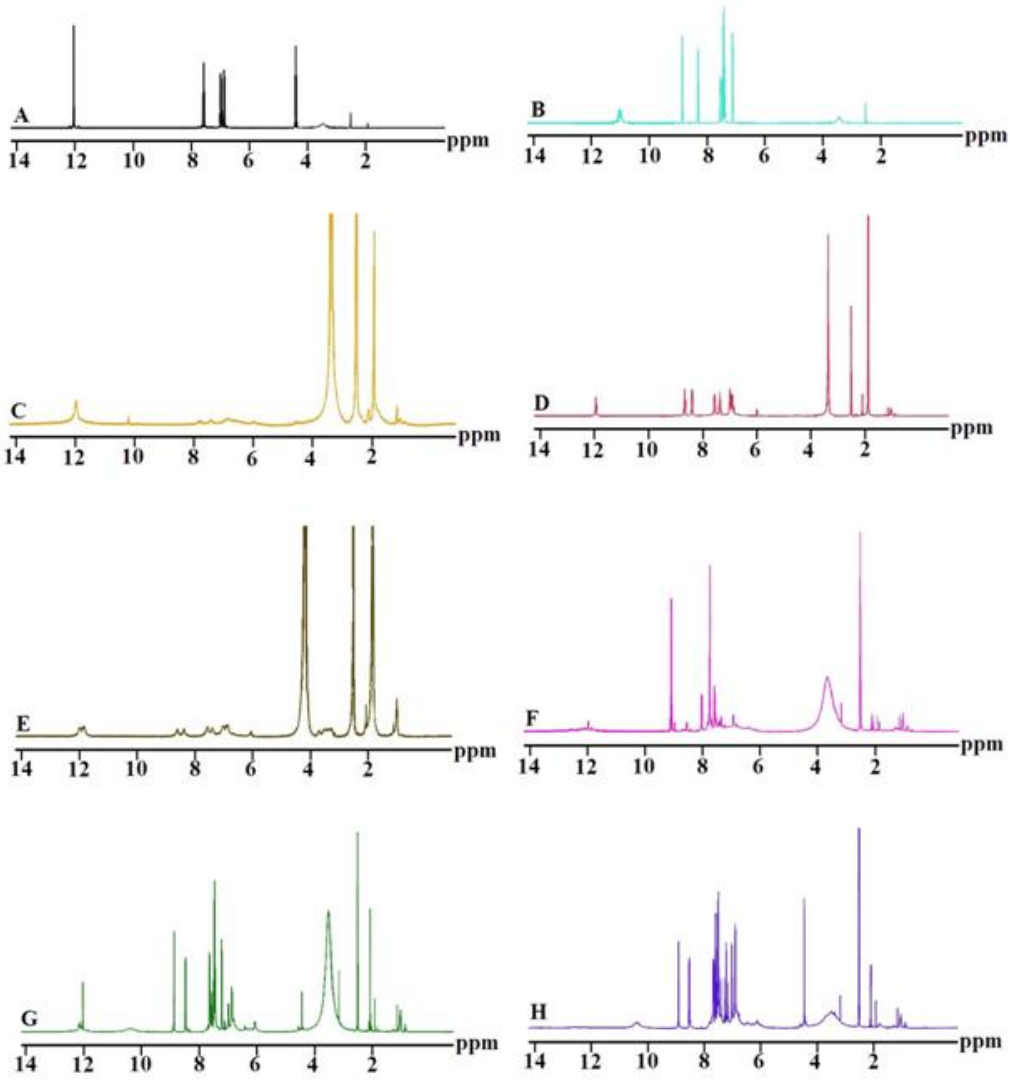

Fig. 3. ^{1}H NMR for (A) Dithr, (B) 8HQ,(C) (1), (D) (2), (E) (3), (F) (4), (G) (5) was recorded in DMSO and (H) complex (2) done in D_2O.

TABLE 4. ^{1}H NMR values (ppm) and tentative assignments for (A) Dithr, 1, 2, 3, 4, 5 and 6.

Assignments	6	5	4	3	2	1	8HQ	Dithr
δH, -CH_2	1.89-2.51	1.91-2.51	1.91-2.51	1.84-2.51	1.88-2.51	1.91-2.51	-	2.51-3.46
δH, H_2O	3.36	3.17-4.45	3.16-4.45	3.17-3.66	3.36	3.34	-	-
δH, -CH aromatic	6.00-8.67	6.88-8.92	6.07-8.90	6.91-8.97	5.98-8.66	6.85-7.98	7.10-8.85	6.85-7.59
δH, OH	-	11.92	12.07	11.96	11.99	11.97	10.5	12.04

Where (6) is Zn(II) complex was done in D_2O.

TABLE 5. The maximum temperature T_{max} (^{o}C) and weight loss values of the decomposition stages for Dithr, 8HQ, (1), (2), (3), (4) and (5).

Compounds	Decomposition	T_{max}(^{o}C)	Weight loss (%)		Lost species
			Calc.	Found	
Dithr	First step		100	99.95	
($C_{14}H_{10}O_3$)	Total loss	274	100	99.95	$3C_4H_2$+2CO+H_2O+H_2
226.23	Residue		-	-	
8HQ	First step		100	99.49	
(C_9H_7NO)	Total loss	176	100	99.49	$2C_4H_2$+NH_3+CO
145.16	Residue		-	-	
	First step		2.99	3.05	H_2O
(1)	Second step	71	27.43	27.22	$4C_2H_2$+NH_3+CO_2
($NiC_{27}H_{29}NO_{11}$)	Third step	250	39.23	39.12	$2C_2H_6$+C_2H_4+3CO+$2O_2$
602.21	Total loss	325	69.65	69.39	
	Residue		30.35	30.61	NiO+9C
	First step	73	27.96	27.55	$4C_2H_2$+NH_3+CO_2
(2)	Second step	327	39.98	39.74	$2C_2H_6$+C_2H_4+3CO+$2O_2$
($ZnC_{27}H_{27}NO_{10}$)	Total loss		67.94	67.29	
590.91	Residue		32.06	32.71	ZnO+9C
	First step		28.75	28.54	$4C_2H_2$+NO+CO+$0.5H_2$
(3)	Second step	99	38.95	39.07	$4C_2H_2$+2HCl+CO_2
($ZrC_{23}H_{19}NO_6Cl_2$)	Total loss	330	67.70	67.61	
567.53	Residue		32.30	32.39	ZrO_2+5C
	First step	84	7.65	7.13	$3H_2O$
(4)	Second step	145	23.37	23.25	$4C_2H_2$+NH_3+CO_2
($LaC_{23}H_{27}NO_9Cl_3$)	Third step	308	30.63	30.88	$2C_2H_4$+CO_2+$0.5H_2O$+HCl+Cl_2
706.73	Total loss		61.65	61.26	
	Residue		38.35	38.74	$LaO_{1.5}$+9C
	First step		8.44	8.41	$4H_2O$
(5)	Second step	79, 151	54.99	55.28	$8C_2H_2$+$0.5H_2$+4HCl+NO+3CO
($ThC_{23}H_{29}NO_{10}Cl_4$)	Total loss	203, 276	63.43	63.69	
853.33	Residue		36.57	36.31	ThO_2+4C

Complex (4) loss hydrated water in the first stage at 84 °C and the coordinated water molecules with 8HQ in the second stage at a maximum temperature 145 °C. The third step of decomposition occurs at 308 °C maximum with a weight loss of 30.88%. This step is associated with the loss of Dithr moiety leaving $LaO_{1.5}$+9C as a final product. The found weight loss associated with each step of decomposition for all steps agree well with the calculated weight loss (Table 5).

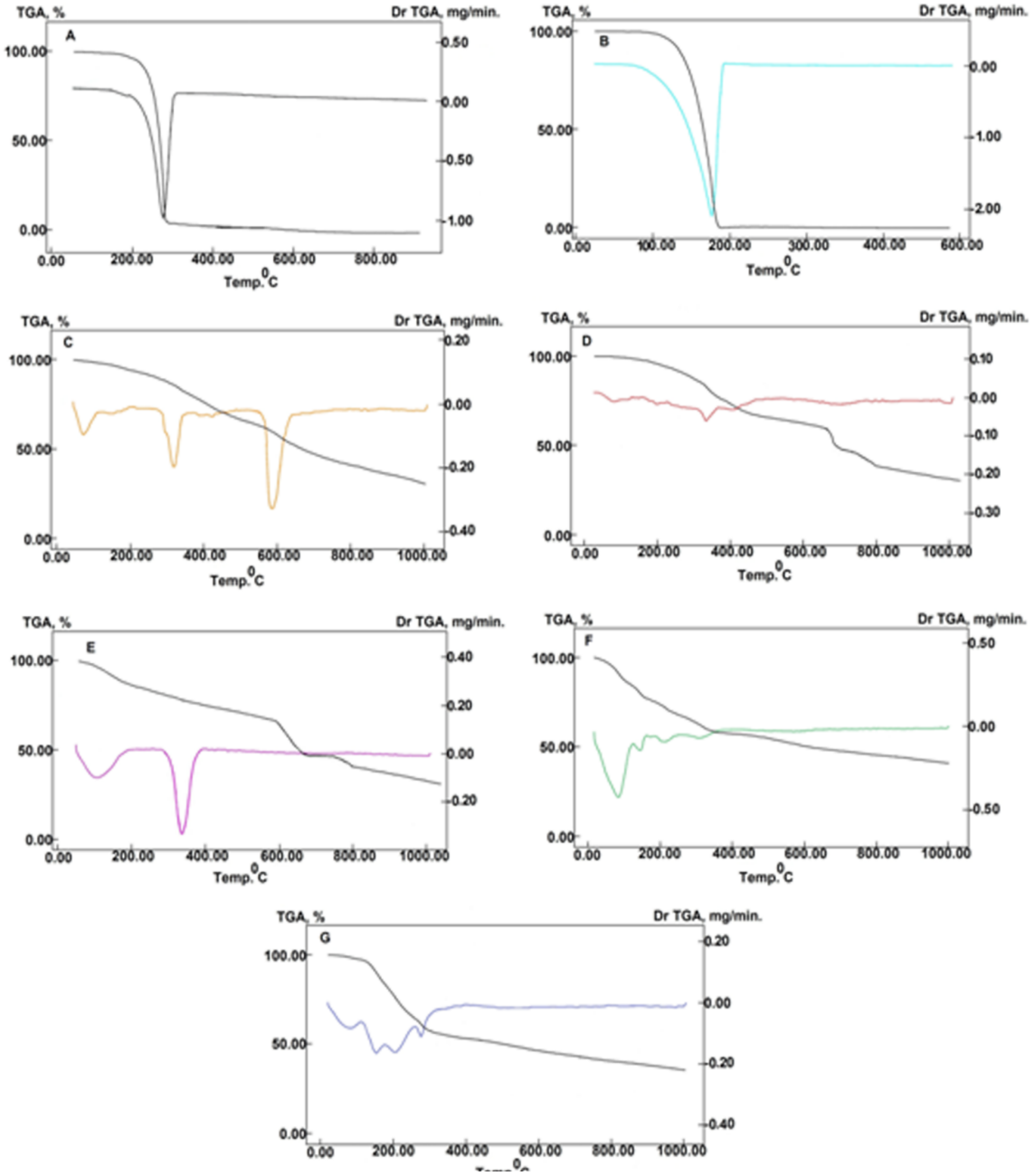

Fig. 4 TGA and DTG diagrams for (A) Dithr, (B) 8HQ, (C) (1), (D) (2), (E) (3), (F) (4) and (G) (5).

The thermal degradation for complex (5) exhibits two main degradation steps. The first stage occurs at 79 and 151 °C maxima, with a weight loss of 8.41% corresponding to the loss of four water molecules. The second step takes place at two maxima: 203 and 276 °C, which accompanied by a weight loss of 55.28%. It is worthy to mention that the found value is in good agreement with the calculated value 54.99% corresponding to the loss of $8C_2H_2$+$0.5H_2$+4HCl+NO+3CO, giving the decomposition product ThO_2+4C.

X-ray diffraction

Although single-crystal X-ray crystallographic investigation is the most precise source of information regarding the structure of a complex, the difficulty of obtaining crystalline complexes renders this method unsuitable for such a study. However, a variety of other techniques could be used with good effect for characterizing the metal complexes as X-ray powder diffraction. So, X-ray powder diffraction (XRD) measurements of Dithr, 8HQ and their complexes were performed (Fig. 5).

Comparative analysis of XRD diagrams of Ni(II), Zn(II), Zr(IV), La(III) and Th(IV) complexes leads to the conclusion that they are identical with the XRD of Dithr and 8HQ, which supports the Dithr and 8HQ molecules are sharing moiety of the resulted complexes. The X-ray diffractions of free ligands have a crystallinity feature which is supported by the peaks distinguished in Fig. 4. The physical checking of XRD diagrams for complexes (1-5) show that they are really a mixture of Dithr and 8HQ with different metal ions as confirmed by the presence of many reflections in comparison with free Dithr and 8HQ. The definite diffraction data, like angle (2θ), interplanar spacing (d value, Angstrom), and relative intensity (%), are summarized in Table 6. The values of 2θ, d value (the volume average of the crystal dimension normal to diffracting plane), full width at half maximum (FWHM) of prominent intensity peak, relative intensity (%), and particle size of complexes are compiled in Table 6. The maximum diffraction patterns of Dithr, 8HQ, Ni(II), Zn(II) and Th(IV) complexes exhibited at 2θ[dvalue(A°)]=8.72(10.14), 14.03(6.31), 8.74(10.11), 9.73(9.09) and 7.41(11.92), respectively. The X-ray diagram of Zr(IV) and La(III) complexes did not showed sharp peaks characteristic to the phases of complex like other complexes. This indicated that Zr(IV) and La(III) complexes to be amorphous in nature. The crystallite size could be estimated from the XRD patterns by applying FWHM of the characteristic peaks using Deby–Scherrer Eq. [29, 30].

$$D=K.\lambda / ß.\cos\theta$$

Where D is the particle size of the crystal gain, K is a constant (0.94 for Cu grid), λ is the X-ray wavelength (0.1542 nm), θ is the Bragg diffraction angle and ß is the integral peak width. The particle size was estimated according to the highest value of intensity compared with the other peaks.

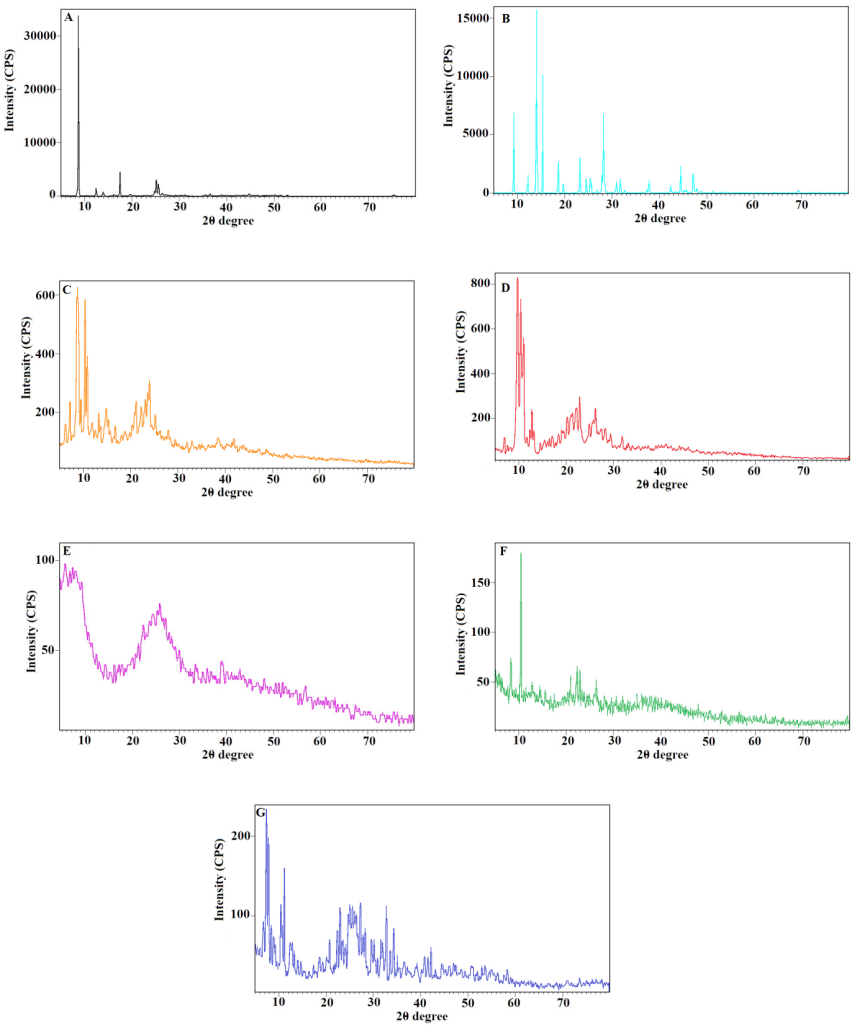

Fig. 5. Powder XRD pattern for (A) Dithr, (B) 8HQ, (C) (1), (D) (2), (E) (3), (F) (4), (G) (5).

TABLE 6 The average crystallite size of Dithr, 8HQ and thier complexes estimated from XRD pattern.

Compounds	2θ (°)	d value (A°)	Relative intensity (%)	Full width at half maximum (FWHM)[a]	Average crystallite size (nm)
Dithr	8.72	10.14	100	0.152	109.38
8HQ	14.03	6.31	100	0.181	68.28
(1)	8.74	10.11	100	0.147	109.14
(2)	9.73	9.09	100	0.112	98.09
(5)	7.41	11.92	100	0.148	128.66

[a] The maximum diffraction patterns according to the highest value of intensity.

Conclusion

Dithr in presence of 8HQ reacts with Ni(II), Zn(II), Zr(IV), La(III) and Th(IV) in acetone and all the complexes are stable at room temperature. The infrared spectra of the complexes showed the presence of the spectral absorption bands in the region 3419-3435 cm^{-1} corresponds to the ν(O-H) vibration in Dithr and 8HQ. The shift of ν(O-H) in all complexes indicated that the chelated of phenolic group with metal ions. The infrared spectrum of 8HQ shows band at 1626 cm^{-1} which attributed to the stretching vibration of ν(C=N). Upon comparison of the IR spectra of the complexes with free ligand, the shift of ν(C=N) to lower frequency values (1551 and 1575 cm^{-1}) confirming that the ligand molecule chelated with the metal ion through the nitrogen atom of pyridine ring.

References

1. Shapiro J. Current Treatment of Alopecia Areata, *J. Invest. Derma. Symp. Proc*. **16**, S42 (2013).

2. Sean, Z., Wu, M. D., Sophie Wang, B. S., Rubina Ratnaparkhi, B. S. Treatment of pediatric alopecia areata with anthralin: A retrospective study of 37 patients. *Ped. Dermatol*. **35**, 817 (2018).

3. Peus, D., Beyerle, A., Rittner, H. L., Pott, M., Meves, A., Weyand, C., Pittelkow M. R. Anti-psoriatic drug anthralin activates JNK via lipid peroxidation: Mononuclear cells are more sensitive than keratinocytes. *J. Invest. Dermatol.* **114**, 688 (2000).

4. Peus, D., Beyerle, A., Vasa, M., Pott, M., Meves, A., Pittelkow, M. R. Antipsoriatic drug anthralin induces EGF receptor phosphorylation in keratinocytes: Requirement for H(2)O(2) generation. *Exp. Dermatol.* **13**, 78 (2004).

5. McGill, A., Frank, A., Emmett, N., Turnbull, D. M., Birch-Machin, M. A., Reynolds, N. J. The anti-psoriatic drug anthralin accumulates in keratinocyte mitochondria, dissipates mitochondrial membrane potential, and induces apoptosis through a pathway dependent on respiratory competent mitochondria. *FASEB J.* **19**, 1012 (2005).

6. Fontánez, N. A., Soler, D. C., McCormick, T. S. Current knowledge on psoriasis and autoimmune diseases. *Psoriasis (Auckl),* **6**,7 (2016).

7. Pietrzak, A., Michalak-Stoma, A., Chodorowska, G., Szepietowski, J. C. Lipid disturbances in psoriasis: An update. *Mediators Inflamm.* **2010**, 1 (2010).

8. Huang, T. H., Lin, C. F., Alalaiwe, A., Yang S. C., Fang, J. Y. Apoptotic or antiproliferative activity of natural products against Keratinocytes for the treatment of psoriasis. *Int. J. Mol. Sci.* **20**, 2558 (2019).

9. John Koo, M. D., Mark Lebwohl, M. D. Duration of remission of psoriasis therapies. *J. Amer. Acad. Derm.* **41**, 51 (1999).

10. Redmond, J. C., Bright, H. A. *Bureau of standards Journal of Research*, **6**, 113 (1930).

11. Geary, W. J. The Use of conductivity measurements in organic solvents for the characterisation of coordination compounds. *Coord. Chem. Rev.* **7**, 81 (1971).

12. Seco, J. M., Quiros, M., Gonzalez Garmendia, M. J. Synthesis, X-ray crystal structure and spectroscopic, magnetic and EPR studies of copper(II) dimers with methoxy-di-(2-pyridyl)methoxide as bridging ligand. *Polyhedron,* **19**, 1005 (2000).

13. Fekri, A., Zaky, R. Solvent-free synthesis and computational studies of transition metal complexes of the aceto- and thioaceto-acetanilide derivatives. *J. Organomet. Chem*. **818**, 15 (2016).

14. Shebl, M. Synthesis and spectroscopic studies of binuclear metal complexes of a tetradentate N_2O_2 Schiff base ligand derived from 4,6-diacetylresorcinol and benzylamine. *Spectrochim. Acta A*, **70**, 850 (2008).

15. Garrido, N. J., Perello, L., Ortiz, R., Alzuet, G., Alvarez, M. G., Canton, E., Gonzalez, M. L., Granda, S. G., Priede, M. P. Antibacterial studies, DNA oxidative cleavage, and crystal structures of Cu(II) and Co(II) complexes with two quinolone family members, ciprofloxacin and enoxacin. *J. Inorg. Biochem*. **99**, 677 (2005).

16. Karipcin, F., Kabalcilar, E. Spectroscopic and thermal studies on solid complexes of 4-(2-pyridylazo)resorcinol with some transition metals. *Acta Chim. Slov*. **54**, 242 (2007).

17. Reddy, P. R., Rajeshwar, S., Satyanarayana, B. Synthesis, characterization of new copper (ii) Schiff base and 1,10 phenanthroline complexes and study of their bioproperties. *J. Photochem.&Photobiol., B: Biology*, **160**, 217 (2016).

18. Zordok, W. A., EL-Shwiniy, W. H., EL-Attar, M. S., Sadeek, S. A. Spectroscopic, thermal analyses, structural and antibacterial studies on the interaction of some metals with ofloxacin. *J. Mol.Struct*. **1047**, 267 (2013).

19. Dhammani, A., Bohra, R., Mohrotra, R. C. Synthesis and characterization of some unique heterocyclic derivatives containing aluminium(III) atoms in different coordination states—4. Reaction of bis(β-diketonato) aluminium(III)-di-μ-isopropoxo-di-isopropoxoaluminium(III) with 8-hydroxyquinoline. *Polyhedron*, **17**, 163 (1998).

20. Bradley, P. G., Kress, N., Hornberger, B. A., Dallinger R. F., Woodruff, W. H. Vibrational spectroscopy of the electronically excited state. 5. Time-resolved resonance Raman study of tris(bipyridine)ruthenium(II) and related complexes. Definitive evidence for the "localized" MLCT state. *J. Am. Chem. Soc*. **103**, 7441 (1981).

21. Shebl, M. Synthesis spectral studies, and antimicrobial activity of binary and ternary Cu(II), Ni(II), and Fe(III) complexes of new hexadentate Schiff bases derived from 4,6-diacetylresorcinol and amino acids. *J. Coord. Chem*. **62**, 3217 (2009).

22. Rochon, F. D., Melanson, R., Macouet, J. P., Belanger-Gariepy, F., Beauchamp, A. L. Preparation and crystal structure of bis(acetato) (*trans*-1,2-diaminocyclohexane)platinum(II). *Inorg. Chim. Acta*, **108**, 17 (1985).

23. Appleton, T. G., Hall, J. R., Ralph, S. F. Reactions of platinum(II) aqua complexes. 3. Multinuclear (nitrogen-15, platinum-195, carbon-13, and proton) NMR study of reactions of aqua and hydroxo complexes with glycine and (methylimino)diacetic acid. *Inorg. Chem*. **24**, 673 (1985).

24. Bennett, M. A., Robertson, G. B., Rokicki, A., Wickramasinghe, W. A. Synthesis, x-ray structural analysis, and thermal decomposition of the platinum(II) carboxylic acid (hydroxycarbonyl) trans-$Pt(CO_2H)(C_6H_5)(PEt_3)_2$. Formation of a diplatinum(II) complex containing carbon dioxide. *J. Am. Chem. Soc*. **110**, 7098 (1988).

25. Sadeek, S. A., El-Attar, M. S., Abd El-Hamid, S. M. Preparation and characterization of new tetradentate Schiff base metal complexes and biological activity evaluation. *J. Mol. Struct*. **1051**, 30 (2013).

26. Sadeek, S. A., Mohammed, S. F., Rashid, N. G. Preparation, spectroscopic characterization, thermal stability and XRD of Some new metal chelates with aceclofenac in presence of 1,10-phenanthroline. *Egypt. J. Chem. 14th Ibn Sina Arab Conf. Heter. Chem. and its App. (ISACHC 2018), Hurgada, Egypt,* **61**, 39 (2018).

27. El-Shwiniy, W. H., Sadeek, S. A. Synthesis, spectroscopic, thermal analyses and biological activity Evaluation of new Zirconium(IV) solid complexes with bidentate lomefloxacin, *Egypt. J. Chem. 14th Ibn Sina Arab Conf. Heter.Chem. and its App. (ISACHC 2018), Hurgada, Egypt,* **61**, 27 (2018).

28. Engelter, C., Knight, C. L., Thornton, D. A. The Infrared and ^{1}H-NMR Spectra of 8-Hydroxyquinoline Adducts of 8-Hydroxyquinoline Complexes of Dioxouranium(VI), Thorium(IV) and Scandium(III). *Spectroscopy Letters*, **22**, 1161 (1989).

29. Quan, C. X., Bin, L. H., Bang, G. G. Preparation of nanometer crystalline TiO_2 with high photo-catalytic activity by pyrolysis of titanyl organic compounds and photo-catalytic mechanism. *Mater. Chem. Phys*. **91**, 317 (2005).

30. Soleymani, R., Aghaei, A., Shahvali, E. A. Synthesis [1-(4-acetylphenyl)-3-(2-methylphenyl)] triazene: NMR, Vibrational, X-ray Crystallography Characterization with HF/ DFT Studies. *Egy. J. Chem.* **61**(2), 361 (2018).

توصيف طيفى و حيود الاشعة السينية لبعض المتراكبات الجديدة مع الدايثرانيول فى وجود ٨ هيدروكسى كينولين

صديق عطية صديق[١]، شريف محمد عبد الحميد[١]، نهاد غالب راشد[٢]

[١]قسم الكيمياء- كلية العلوم- جامعة الزقازيق- الزقازيق- مصر

[٢]وزارة التعليم- بابل- العراق

يهدف هذا البحث الحالى إلى تحضير متراكبات جديدة ناتجة عن تفاعل الدايثرانيول فى وجود ٨ هيدروكسى كينولين مع بعض العناصر الإنتقالية مثل النيكل الثنائى والزنك الثنائى والزركونيوم الرباعى واللانثانوم الثلاثى والثوريم الرباعى. تم توصيف التركيب الجزيئى للمتراكبات المتكونة باستخدام التحاليل (قياس درجة الانصهار والخواص الكهربية وقياسات العزم المغناطيسى والتحليل العنصرى والأشعة تحت الحمراء والأشعة فوق البنفسجية وأطياف الرنين النووى المغناطيسى البروتونى وحيود الاشعة السينية) بالإضافة إلى التحليل الوزنى الحرارى. وقد أسفرت نتائج الخواص الكهربية للمتراكبات الذائبة فى ثنائي ميثيل سلفوكسيد أن المتراكبات لها خصائص توصيلية بنسب مختلفة. قياسات العزم المغناطيسى للنيكل الثنائى تكافىء ٣,١ مغنطون بور بنية مشوهة ثمانية السطوح. وقد أثبتت التحاليل الوزنية الحرارية الصيغ الكيميائية لهذه المتراكبات و أكدت عمليات التكسير الحرارى منتهية بتكوين اكسيد المعدن مع ذرة كربون. وقد أظهرت دراسة الأشعة تحت الحمراء الطيفية أن هناك حدوث تغيير فى الإمتصاصة الخاصة بمجموعات الهيدروكسيل والازوميثين فى جميع المتراكبات التى أوضحت أن ٨ هيدروكسى كينولين يتفاعل مع ايونات المعدن من خلال ذرة الأكسجين لمجموعة الفينول وذرة النيتروجين لحلقة البيريدين. وقد أظهر تحليل حيود الأشعة السينية للمركبات أن الدايثرانيول و ٨ هيدروكسى كينولين والمتراكبات الناتجة لها قمم بلورية ماعدا متراكبات الزركونيوم الرباعى و اللانثانوم الثلاثى.